J Stat Phys (2008) 132: 945–955
DOI 10.1007/s10955-008-9573-4

Mode-Locking in Driven Disordered Systems as a Boundary-Value Problem

William Kung · M. Cristina Marchetti

Received: 19 January 2008 / Accepted: 21 May 2008 / Published online: 11 June 2008

Abstract We study mode-locking in disordered media as a boundary-value problem. Focusing on the simplest class of mode-locking models that consists of a single driven overdamped degree-of-freedom, we develop an analytical method to obtain the shape of the Arnol'd tongues in the regime of low AC-driving amplitude or high AC-driving frequency. The method is exact for a scalloped pinning potential and easily adapted to other pinning potentials. It is complementary to the analysis based on the well-known Shapiro's argument that holds in the perturbative regime of large driving amplitudes or low driving frequency where the effect of pinning is weak.

Keywords Mode-locking · Boundary-value problem · Arnol'd tongues

1 Introduction

The phenomenon of mode-locking is a general feature of nonlinear dynamical systems. It consists of a resonant response to an external periodic force that occurs when a characteristic frequency of the driven system matches or *locks onto* the driving frequency. In the mode-locked region, the system traces periodic orbits in phase space. Outside the region of mode locking, the system may follow quasiperiodic orbits or march towards the onset of chaos.

Examples of systems that exhibit the mode-locking behavior abound in nature. In 1665, Huygens discovered the spontaneous synchronization of swinging pendulum clocks in close proximity to one another. On the celestial scale, the moon's period of rotation locks onto its period of revolution about the Earth in a 1:1-ratio, so it always presents the same face to observers on Earth. The rotation of Mercury is also locked onto the Sun such that there are three rotations for every two orbits, thereby constituting a scenario of 3:2-mode locking. Mode-locking to external periodic stimuli is also a common feature in biology. Examples include

W. Kung (✉)
Department of Materials Science and Engineering, Northwestern University, Evanston, IL 60208, USA
e-mail: w-kung@northwestern.edu

M.C. Marchetti
Department of Physics, Syracuse University, Syracuse, NY 13244, USA

the cell cycle found in budding yeast [1], the swimming and heartbeat networks of medicinal leeches [2], as well as the rhythmic behavior produced by neuronal networks [3]. The mode-locking behavior is also relevant in such diverse phenomena as vortex shedding [4], singing sand dunes [5], and multimode lasers [6–8]. In condensed-matter physics, Josephson junction arrays [9], driven superconducting vortices [10–12], as well as charged-density waves (CDW) [14–20] provide convenient settings for studying the phenomenon of mode-locking.

Mathematicians have long used the language of *maps* to describe trajectories followed by dynamical systems in phase space from which they would infer their associated physical properties. In particular, circle maps [21, 25], along with the mathematical tools of bifurcation theory and return map, lay the foundation for much of the theoretical modeling and analysis of mode-locking phenomena. Though based on previous studies [22, 23], the correspondence between circle maps and an overdamped particle in a periodic potential is not simple. Conceptually, the simplest evolution equation that yields mode-locking behavior consists of a single overdamped degree-of-freedom (DOF) ϕ in a periodic *pinning* potential $V_p(\phi)$ of strength h, driven by an external periodic force of frequency ω. The dynamics is described by the equation

$$\frac{d\phi}{dt} = F_0 + F_1 \cos\omega t + F_p(\phi), \tag{1}$$

where $F_p(\phi) = -h\frac{dV_p(\phi)}{d\phi}$ is the pinning force. Mode-locking behavior occurs when the time-averaged velocity locks on to a rational multiple of the external driving frequency:

$$\begin{aligned}\left\langle \frac{d\phi}{dt} \right\rangle_{\text{cycle}} &\equiv \int_{2\pi/\omega} \frac{1}{2\pi/\omega} \frac{d\phi}{dt} \\ &= F_0 + \left\langle F_p \right\rangle_{\text{cycle}} \equiv \omega_d = \frac{p}{q}\,\omega \end{aligned} \tag{2}$$

for a region of nonzero area in the (F_0, F_1)-parameter space. The regions in the (F_0, F_1)-parameter space where mode-locking occurs are known as Arnol'd tongues.[1] The time-averaged velocity exhibits the behavior of a devil's staircase (DS): there exists a mode-locked plateau corresponding to each rational p/q. While there have been much work on the fractal dimensionality in the set of gaps between the mode-locked steps in the staircase [24–28], most results concerning the width of the corresponding mode-locked steps have relied upon an approximate method proposed by Thorne et al. [30] that generalizes an argument originally due to Shapiro [29]. Thorne's method, introduced in the context of a single-particle model of CDW, is based on the identification of the mode-locked steps with the corresponding regions of minima in the pinning energy for the system.

Early analytical results for specific pinning potentials have indicated, however, that the correspondence between a single overdamped particle in a periodic pinning potential and the circle map may not be simple and that Thorne's "pinning energy" approximation may be qualitatively incorrect. The simplest case where exact analytical results are available is a single overdamped DOF in a cosine pinning potential, $V_p(\phi) = h\cos\phi$. It was shown in [22] and [23] that, for the cosine potential, there are no subharmonic mode-locked plateaus (corresponding to $q \neq 1$). In addition, the Arnol'd tongues are symmetric with respect to the mirror axis centered at the apex of the tongue and pinch to zero width for all parameters in the phase space, as shown in Fig. 1. The condition wherein the mode-locked steps occur in

[1] See, for example, Fig. 3 in [24], or see Figs. 3 and 4 in [3].

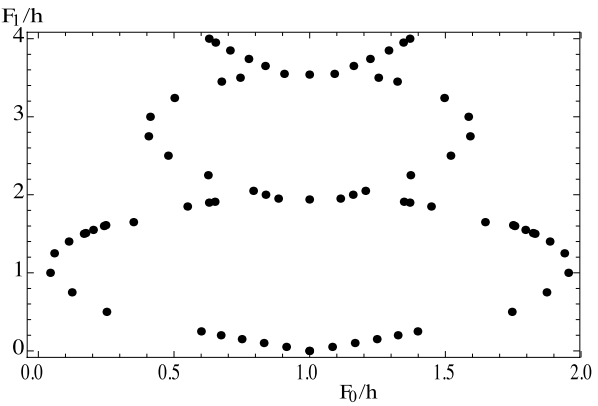

Fig. 1 1:1 Arnold tongue for pure cosine pinning potential

regions where the pinning energy in the mode-locked state is lower than that in the unlocked state is identically satisfied for the system of a single particle in a pure cosine pinning potential. However, as shown below, this condition is only necessary and not sufficient condition of stability of the mode-locked state for a more generic periodic pinning potential. In fact the "pinning energy"-argument predicts the existence of both harmonic and subharmonic steps for a general periodic pinning potential containing higher harmonics [29, 30]. This is in contrast to the exact results obtained by Azbel and Bak for a single overdamped degree of freedom in a pinning potential consisting of a series of delta functions that showed explicitly the absence of subharmonic steps [31]. Thus, the work of Azbel and Bak provided strong early evidence that the approximate "pinning-energy" method may be qualitatively incorrect.

In this paper, we demonstrate how this method fails to reproduce the mode-locking behavior in details even for the 1:1-step. In particular, we re-examine the single DOF model for various pinning potentials and show that the cosine pinning is special. For a generic periodic pinning potential containing higher harmonics, the tongues are, in general, asymmetric and do not pinch to zero. Numerics have shown that, in extended systems consisting of many coupled DOFs, the Arnol'd tongues are generally asymmetric and never pinch to zero width. This more-complex shape of the Arnol'd tongues may be the result of the collective behavior of many coupled degrees of freedom; it can arise even for a single particle provided that the pinning potential differs from a simple cosine one. Of course in an extended system, collective effects renormalize the pinning potential, so even a bare cosine pinning would yield asymmetric Arnol'd tongues. In what follows, we show that for generic pinning potential the Shapiro's method always fails at small F_1, where the asymmetry of the Arnol'd tongue is the most apparent. For the exemplary case of scalloped potential, we develop an exact analytical method for the calculation of the mode-locking behavior of a single DOF for F_1 small enough so that the single DOF does not hop from one scallop to the next. This is precisely the regime where the Shapiro's argument always fails. Our analytical solution for small F_1 also provides dynamical constraints that are both necessary and sufficient for the full determination of the mode-locked step widths.

Thus, this work serves as a starting point in our effort to construct a mean-field theory for the general phenomenon of mode-locking in extended media that is amenable to analytical analysis in useful limits. To do so, we must first test analytical approximations at the single-particle level and identify a simple, yet generic, pinning potential as our prototypical starting point. To achieve these two initial goals, we study in detail the case of 1:1-mode locking and

consider two specific periodic pinning potential $G[\phi]$: the scalloped parabolic potential and an impure cosine potential (consisting of more than one harmonic). In Sect. 2, we will review Shapiro's method for calculating the width of mode-locked steps. We will then consider the mode-locking dynamics of one particle in the scalloped parabolic pinning potential in Sect. 3. This form of potential has the advantage of permitting exact analytical solution in the no-hopping regime. In Sect. 4, we will repeat our analysis for the impure cosine pinning potential. Section 5 concludes our paper.

2 Shapiro's Method in Calculating Mode-Locked Step Widths

Adapting an argument proposed by Shapiro [29], Thorne *et al.* computed the width of the harmonic and subharmonic mode-locked steps for the one-DOF model of CDW given in (1) [30]. While their calculation explains the occurrence of mode-locking in terms of the lowering of the pinning energy, their results do not agree with numerical results for the shape of the Arnol'd tongues in the regime of low AC-driving amplitude or high AC-driving frequency. This regime corresponds to the case where the particle dynamics is confined to one period of the pinning potential. To show how Shapiro's method fails in this regime, we first review the calculation of Thorne et al. [30].

It is instructive to first consider the single DOF model of (1) for a cosine pinning potential. We note that in the absence of pinning the equation of motion has the exact solution $\phi(t) = F_0 t + \frac{F_1}{\omega} \sin \omega t + \phi_0$, with ϕ_0 a constant, which gives the trivial result $\omega_d = F_0$. In the presence of pinning we let

$$\phi(t) = \omega_d t + \frac{F_1}{\omega} \sin \omega t + \phi_0(t), \tag{3}$$

with ω_d and $\phi_0(t)$ to be determined. We note that (1) contains two characteristic frequency scales: the frequency ω of the external drive and the frequency h of temporal variations of the phase due to the pinning potential. In the limit of large drive, the particle moves rapidly over the pinning potential and the temporal variations due to pinning are consequently small. Following [30] we then look for a solution where $\phi_o \approx$ constant, independent of time. We expect this approximation will apply for large F_1 and weak pinning. It turns out to be essentially exact for a simple cosine pinning potential, but it fails for small values of F_1 for arbitrary periodic pinning. Substituting (3) into (1), utilizing the Bessel function summation formula

$$\exp\left[-\imath \left(\frac{F_1}{\omega}\right) \sin \omega t\right] = \sum_{p=-\infty}^{\infty} J_p\left(\frac{F_1}{\omega}\right) \exp(-\imath p \omega t), \tag{4}$$

and averaging over a cycle, we obtain

$$\omega_d = F_0 + \langle F_p \rangle_{\text{cycle}}, \tag{5}$$

$$\langle F_p \rangle_{\text{cycle}} = h \sin \phi_0 \sum_{\substack{p=1 \\ (\omega_d = p\omega)}}^{\infty} (-1)^p J_p(F_1/\omega), \tag{6}$$

where the sum is over all p such that $\omega_d = p\omega$. Similarly the mean pinning energy is given by

$$\langle V_p \rangle_{\text{cycle}} = h \cos\phi_0 \sum_{\substack{p=1 \\ (\omega_d = p\omega)}}^{\infty} (-1)^p J_p(F_1/\omega). \tag{7}$$

A mode-locked state occurs when ω_d in (5) can be kept constant (and equal to $p\omega$) for a range of values of F_0 and F_1 by adjusting the phase ϕ_0. For a cosine pinning potential the range of ϕ_0 that renders $\omega_d =$ constant is identical to the range of ϕ_0 where $\langle V_p \rangle_{\text{cycle}} < 0$. In this case the region of parameters where the system is mode-locked coincides with the region where the energy of the mode-locked state is lower than that of the unlocked state. This is not, however, the case for arbitrary pinning potential, as we will see below. In general the condition that energy of the mode-locked state be lower than that of the unlocked state is necessary for their stability of the mode-locked state, but not sufficient (see Fig. 5 below). For pure cosine pinning case only harmonic steps are obtained. The $p/1$ step occurs for a range $(\Delta F_0)_{p/1}$ of values of F_0 given by $(\Delta F_0)_{p/1} = 2h|J_p(F_1/\omega)|$. The Arnol'd tongues for this case are shown in Fig. 1.

Thorne and collaborators adapted this argument to an arbitrary periodic pinning potential that can be expressed as a Fourier sum:

$$V_p(\phi) = \frac{a_0}{2} + \sum_{q=1}^{\infty} a_q \cos q\phi, \tag{8}$$

Proceeding as in the single cosine case, using again the Bessel summation formula and averaging over a cycle, we find that ω_d is determined by (5), where the time-averaged pinning force is zero unless $\omega_d = p\omega/q$, for which

$$\langle F_p \rangle_{cycle} = 2 \sum_{q=1}^{\infty} \sum_{p=-\infty}^{\infty} q a_q J_p \left(\frac{q F_1}{\omega} \right) \sin q\phi_0. \tag{9}$$

Thus, for a given F_1, the constant phase ϕ_0 can be adjusted to compensate changes in F_0 such that the time-average phase velocity ω_d stays locked to rational values of the external driving frequency. Furthermore, (9) suggests that the width of the Shapiro steps oscillates with F_1, which has indeed been observed in experiments [12, 13]. These authors further assumed that the range of parameters where the system is mode-locked coincides with those where the mean pinning energy in the mode locked state is lower than its value $a_0/2$ in the unlocked state, i.e.,

$$\delta \langle V_p \rangle_{cycle} = \sum_{q=1}^{\infty} \sum_{p=-\infty}^{\infty} a_q J_p \left(\frac{q F_1}{\omega} \right) \cos(q\phi_0) < 0. \tag{10}$$

The mean pinning force given by (9) cancels the DC drive F_0 in a range $-\phi_p(F_0, F_1) \leq \phi_0 \leq \phi_p(F_0, F_1)$. The condition that $\phi_p(F_0, F_1) \in [0, 2\pi]$ can then be used to determine the boundaries of the mode-locked regions in the (F_0, F_1) plane. Thorne et al. use the condition $\delta \langle V_p \rangle_{cycle} < 0$ to determine the Arnol'd tongues. The latter holds for a range $-\phi_m(F_0, F_1) \leq \phi_0 \leq \phi_m(F_0, F_1)$. For pure cosine pinning $\phi_m(F_0, F_1) = \phi_p(F_0, F_1)$. For arbitrary pinning potentials $\phi_m(F_0, F_1) \geq \phi_p(F_0, F_1)$, resulting in an overestimate of the mode-locked regions. Regardless of the condition used for mode-locking, a consequence

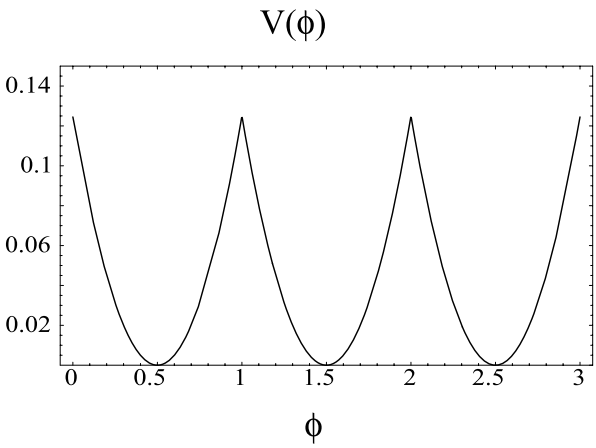

Fig. 2 The scalloped parabolic pinning potential, defined by (11)

of (9) and (10) is that each Arnol'd tongue is symmetric about a central axis for any periodic pinning potential. In the case of 1:1-mode locking, the tongue is symmetric about the axis $F_0 = 1$, since $J_p(0) = 0$ for all $p \neq 0$ and $J_0(0) = 1$ assuming appropriate normalization. For the 1:1-mode locking case, we will show explicitly, via exact numerical calculations, that this symmetry of Arnol'd tongue is violated in the regime where the influence of AC-drive is large, *i.e.* when the drive amplitude F_1 is small or the drive frequency ω is small (*cf.* Fig. 4), for two specific cases of the periodic pinning potential corresponding to the scalloped parabolic and the impure cosine pinning.

3 Scalloped Parabolic Pinning Potential

We first consider the case of scalloped parabolic pinning, whose potential can be expressed either in terms of the floor function, $\lfloor x \rfloor$, defined as the largest integer less than or equal to its argument x, or as a Fourier series:

$$V_{\text{scalloped}}(\phi) = \frac{1}{2}\left(\phi - \lfloor \phi \rfloor - \frac{1}{2}\right)^2 \tag{11}$$

$$= \frac{1}{24} + \sum_{q=0}^{\infty} \frac{1}{2\pi^2 q^2} \cos 2\pi q \phi. \tag{12}$$

A plot of the scalloped parabolic potential is shown in Fig. 2. In this case the double sum in the expression for the time-averaged pinning force, (9), reduces to a single infinite sum over terms for which $p = q$. Using (12), the cycle-averaged pinning force is given by:

$$\langle F_p(\phi_0) \rangle_{cycle} = \sum_{q=0}^{\infty} \frac{1}{\pi q} J_q(q F_1) \sin 2\pi q \phi_0. \tag{13}$$

For the scalloped pinning potential of Fig. 2 the pinning force is piece-wise linear and the dynamics of the driven particle can be solved exactly within each period of the pinning potential. This solution is expected to be exact for small values of F_1, provided that the

particle does not hop from one scallop to the next on the time scale of the external drive. Within one period (1) is simply

$$\frac{d\phi}{dt} + \phi = \left(F_0 + \frac{1}{2}\right) + F_1 \cos 2\pi t. \tag{14}$$

For simplicity we discuss in detail only mode-locked steps with $p = 1$. In this case (14) must be solved with the boundary conditions

$$\phi(t_J + nT) = 0, \tag{15}$$

$$\phi(t_J + (n+1)T) = 1, \tag{16}$$

where $T = 2\pi q/\omega$. The jump time t_J plays the role of the constant phase ϕ_0 in the previous section. Equation (15) determines the constant of integration for our first-order ODE, while (16) yields the relationship between F_0 and F_1 corresponding to mode-locking. This can be rewritten as

$$\frac{1}{1 - e^{-1}} = \left[F_0 + \frac{1}{2} + \frac{F_1}{h^2 + \omega^2}(\cos 2\pi t_j - 2\pi \sin 2\pi t_j)\right]. \tag{17}$$

The condition that the values of t_J in (17) must be in $[0, T]$ determines the boundaries $F_1(F_0)$ of the Arnol'd tongues, given by

$$F_1 \geq \pm\sqrt{1 + (2\pi)^2}\left(\frac{1}{1 - e^{-1}} - F_0 - \frac{1}{2}\right). \tag{18}$$

These are the straight lines shown in Fig. 3, along with the complete Arnol'd tongues for the 1:1 step obtained by exact numerics. Clearly the analytical solution yields the exact value of F_0 for the onset of mode-locking at $F_1 = 0$ and also does an excellent job of fitting the exact Arnol'd tongues for small F_1, where the driven particle remains within a single scallop. In contrast, Shapiro's argument fails most severely precisely in this region of small F_1, as apparent from Fig. 4 where the Arnol'd tongues obtained for the 1:1 mode-locked step by the Shapiro argument (triangles) are compared to the exact solution (diamonds). As mentioned in Sect. 2, Shapiro's method predicts symmetrical oscillation about the axis $F_0 = 1$. However, exact numerical solution reveals that the 1:1-mode locked step, in fact, originates from $F_0 \approx 1.1$. This difference arises because the Shapiro method is essentially a perturbation theory about the high velocity state and becomes exact at large drives and very weak disorder. On the other hand for fixed driving frequency ω and small AC-drive amplitude F_1, or conversely fixed F_1 and high frequency the driving force has only a weak effect and pinning dominates. In this region the time-averaged velocity is well approximated by the instantaneous velocity. This fact underlies our approximation scheme in which we solve exactly for the instantaneous dynamical solution for the CDW phase $\phi(t)$, assuming that the particle does not hop over any one scallop in the periodic pinning potential. Neglecting the effect of scallop-hopping simplifies the dynamics considerably, as the elimination of the associated nonlinearity permits analytically tractable solutions. This method is complementary to the one developed by Shapiro. Our method can be readily generalized to other harmonic and subharmonic mode-locking steps that involve no hopping between scallops and thus satisfy the constraint $p = 1$.

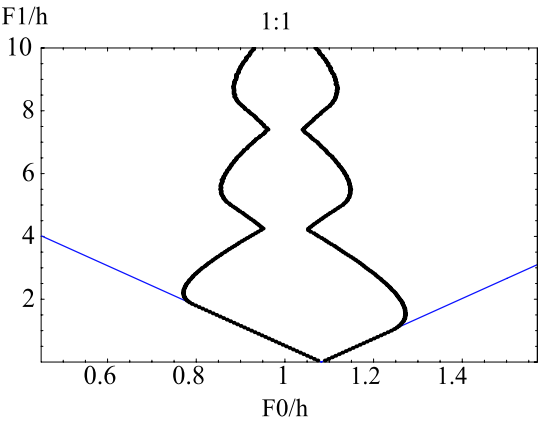

Fig. 3 1:1 Arnold tongue for scalloped parabolic pinning potential: numerical method versus "exact" method for small F_1

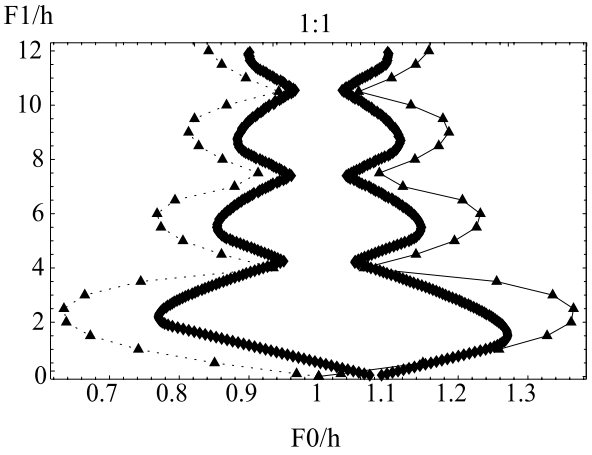

Fig. 4 Plot of Arnol'd tongue for 1:1 mode-locking step with the scalloped parabolic pinning potential. *Black triangles* represent data points obtained from the zeros of the pinning energy using Thorne's method. Numerically, the first 100 terms of the sum were included in our summation over the Bessel functions. The *black diamonds* represent data from numerical results

4 Impure Cosine Pinning Potential

For a cosine pinning potential the width of mode-locked steps pinches to zero periodically at finite values of the AC-driving amplitude, F_1. This is well explained by Shapiro's argument [30] based on its expression of the time-averaged pinning potential: since the time-averaged pinning force has only one term for any particular values of p and q and it is a consequence of the fact that pinning potential contains only a single harmonic in its Fourier series. To see this point explicitly, we compare the two cases of a pure cosine pinning potential function and of an *impure* cosine, consisting of a sum of two different harmonics:

$$V_{\text{cosine}}(\phi) = \frac{1}{2\pi}\cos 2\pi\phi, \tag{19}$$

$$V_{\text{impure}}(\phi) = \frac{1}{2\pi}\cos 2\pi\phi + \frac{0.1}{4\pi}\cos 4\pi\phi. \tag{20}$$

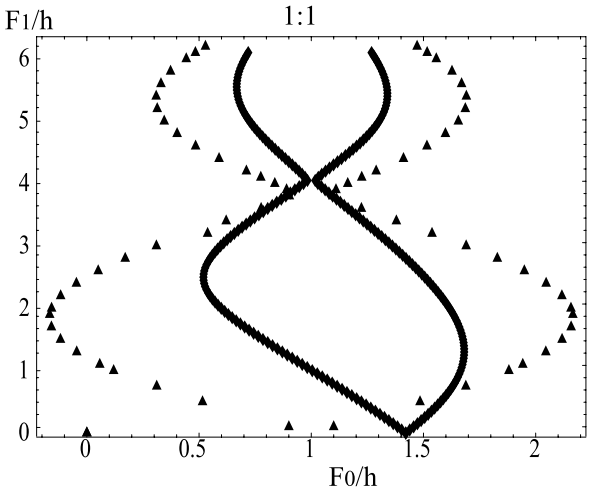

Fig. 5 Plot of the impure cosine pinning potential consisting of a sum of two harmonics. *Gray triangles* represent data points obtained from the zeros of the pinning energy using Thorne's method. The *black diamonds* represent data from numerics

Again we are focusing on 1:1-mode locked steps. For the impure cosine pinning, the time-averaged pinning force is

$$\langle F_p(\phi_0)\rangle \sim J_1(F_1)\sin 2\pi\phi_0 + 0.1J_2(2F_1)\sin 4\pi\phi_0 \tag{21}$$

It is apparent from Fig. 5 that the addition of a small harmonic is sufficient to give a finite width to the tongues for all nonzero values of F_1. Again Shapiro's method clearly fails at small F_1. To analyze the dynamics in this region, we assume that there is no particle-hopping and use the analytical method discussed in the previous section. To do this we fit the impure cosine pinning potential to a parabola over one cycle. Using Mathematica, we find that the fitted pinning potential yields $V^F_{\text{cosine}}(\phi) = 0.186 - 1.17\phi + 1.19\phi^2$, or equivalently, a scalloped parabolic pinning potential with a pinning strength of $h \approx 2.39$ over the same cycle. The resulting comparison plot of the numerically obtained Arnol'd tongue for 1:1-mode locking and the "V"-shaped asymptotes obtained analytically in the no-hopping approximation is shown in Fig. 6. Again, there is remarkable agreement between our analytical approximation and the exact numerical solution in the small-drive regime.

To further clarify the role of the no-hopping approximation used in our analytical calculation, we note that in obtaining (18), we implicitly assume that $|\phi(t)| \leq 1$, for $t \in [0, 2\pi]$. Self-consistency of our solution is then imposed by looking for the set of points in the region defined by (18) that explicitly satisfy $|\phi(t)| \leq 1$ for $t \in [0, 2\pi]$. As shown in Fig. 7, the region of (F_0, F_1), bounded by black circles, which explicitly satisfies the constraint $|\phi(t)| \leq 1$ is an excellent approximation to the lopsided pear-shaped region of the Arnol'd-tongue for $F_1 < 4$. Beyond this region, the particle presumably hops over more than one scallop per drive period, and our analytical approximation would no longer apply.

5 Conclusion

In summary, we have developed a simple analytical method to obtain the shape of the Arnol'd tongues in the regime of small AC-driving amplitude F_1 or high-driving frequency, where the driven particle does not hop between different periods of the driving potential within one period of the drive. This method is complementary to the perturbative one based

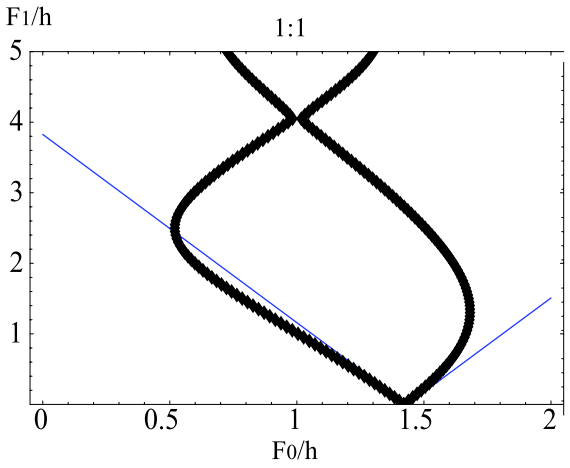

Fig. 6 Shape of the Arnol'd tongue for the 1:1 mode-locking step for an impure cosine pinning potential. The *diamonds* are exact numerical results and the *V-shaped straight lines* are the analytical approximation in the no-hopping regime, corresponding to the limit of small drive/high frequency

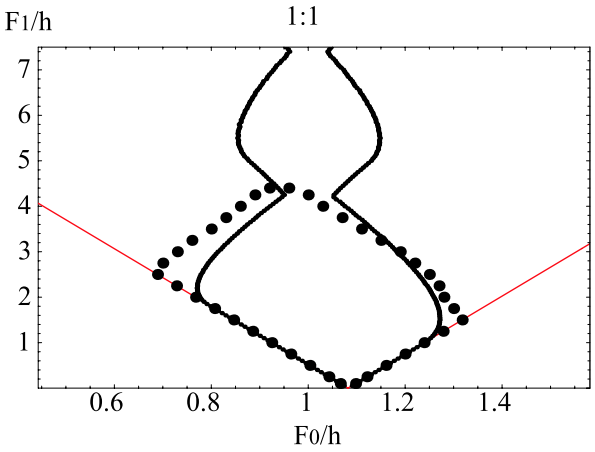

Fig. 7 The shape of the Arnol'd tongue for the 1:1 mode-locking step for a scalloped parabolic pinning potential. The *solid line* are exact numerical results and the (red online) *V-shaped straight lines* correspond to the analytical approximation in the no hopping regime. The region bounded by the *black circles* are points of (F_0, F_1) which are explicitly checked to satisfy the constraint of $|\phi(t)| \leq 1$

on Shapiro's argument [29, 30] that applies in the large F_1 or low frequency regime. The method is exact for a scalloped pinning potential and is easily adapted to other pinning potentials by a simple fit. Our method is easily adapted to the analysis of p/q mode-locking steps for arbitrary q and $p = 1$.

As mentioned in the Introduction, the motivation of this work was to develop simple methods for the analysis of mode-locking steps that will serve as the starting point for the development of a mean-field theory of mode-locking in systems composed of many interacting many degrees of freedom. We hope to do this by combining the no-hopping approximation for the analysis of the low drive regime with the Shapiro argument for the study of the high-drive region. It would also be interesting to consider numerically the crossover limit to the large driving limit. Finally, while the phenomenon of mode-locking is pervasive in dynamical systems, each subfield has developed its own set of theoretical tools, often inspired and required by real-world applications. Despite past attempts [32], a consensus is still lacking in regard to a unifying formalism in the description of mode-locking. It is our further hope that our results would illuminate aspects of mode-locking, which are still not well understood and which would merit further study.

Acknowledgements We would like to thank Alan Middleton for helpful discussions. This work was supported by NSF Grants DMR-0305497 and DMR-0705105.

References

1. Cross, F.R., Siggia, E.D.: Phys. Rev. E **72**, 021910 (2005)
2. Calabrese, R.L., de Schutter, E.: Trends Neurosci. **15**, 439 (1992)
3. Coombes, S., Bressloff, P.C.: Phys. Rev. E **60**, 2086 (1999)
4. Mureithi, N.W., Masaki, R., Kaneko, S., Nakamura, T.: J. Press. Vessel Technol. **363**, 19 (1998)
5. Andreotti, B.: Phys. Rev. Lett. **93**, 238001 (2004)
6. Haus, H.A.: IEEE J. Sel. Top. Quantum. Electron. **6**, 1173 (2000)
7. Gat, O., Gordon, A., Fischer, B.: New J. Phys. **7**, 151 (2005)
8. Moores, J.D.: Opt. Lett. **26**, 87 (2001)
9. Das, S., Datta, S., Sahdev, D.: Phys. D **101**, 333 (1997)
10. Karapetrov, G., Fedor, J., Iavarone, M., Rosemann, D., Kwok, W.K.: Phys. Rev. Lett. **95**, 167002 (2005)
11. Kokubo, N., Besseling, R., Vinokur, V.M., Kes, P.H.: Phys. Rev. Lett. **88**, 247004 (2002)
12. Besseling, R., Benningshof, O., Kokubo, N., Kes, P.H.: Phys. C **408**, 581 (2004)
13. Lübbig, H., Luther, H.: Rev. Phys. Appl. **9**, 29 (1974)
14. Grüner, G.: Rev. Mod. Phys. **60**, 1129 (1988)
15. Fukuyama, H., Lee, P.A.: Phys. Rev. B **17**, 535 (1978)
16. Lee, P.A., Rice, T.M.: Phys. Rev. B **19**, 3970 (1979)
17. Kolton, A.B., Dominguez, D., Gronbech-Jensen, N.: Phys. Rev. Lett. **86**, 4112 (2001)
18. Fisher, D.S.: Phys. Rev. Lett. **50**, 1486 (1983)
19. Fisher, D.S.: Phys. Rev. B **31**, 1396 (1985)
20. Alstrom, P., Ritala, R.K.: Phys. Rev. A **35**, 300 (1987)
21. Pradhan, G.R., Chatterjee, N., Gupte, N.: Phys. Rev. E **65**, 046227 (2002)
22. Waldrum, J.R., Wu, P.H.: J. Low Temp. Phys. **47**, 363 (1982)
23. Renne, M.J., Polder, D.J.: Rev. Phys. Appl. **9**, 25 (1974)
24. Wiersig, J., Anh, K.H.: Phys. E **12**, 256 (2002)
25. Jensen, M.H., Bak, P., Bohr, T.: Phys. Rev. A **30**, 1960 (1984)
26. Halsey, T.C., Jensen, M.H., Kadanoff, L.P., Procaccia, I., Shraiman, B.I.: Phys. Rev. A **33**, 1141 (1986)
27. Biham, O., Mukamel, D.: Phys. Rev. A **39**, 5326 (1989)
28. Wenzel, W., Biham, O., Jayaprakash, C.: Phys. Rev. A **43**, 6550 (1991)
29. Shapiro, S., Janus, A., Holly, S.: Rev. Mod. Phys. **36**, 223 (1964)
30. Thorne, R.E., Tucker, J.R., Bardeen, J., Brown, S.E., Gruner, G.: Phys. Rev. B **33**, 7342 (1986)
31. Azbel, M.Y., Bak, P.: Phys. Rev. B **30**, 3722 (1984)
32. MacKay, R.S.: J. Nonlinear Sci. **4**, 301 (1994)